ISBN: 978-628-96613-1-6. ISSN: 2414-6390. Digital Object Identifier: https://dx.doi.org/10.18687/LACCEI2025.1.1.1111

Experimental Aerodynamic Performance of the SG6043 Airfoil with Flow Control Devices

Gustavo Richmond-Navarro[1]; Isaac Barrios Campos[1]; Iván Araya Meneses[1];
Maximino Jiménez-Ceciliano[1]; Juan José Montero-Jiménez[1]
[1]*Tecnológico de Costa Rica, Costa Rica* grichmond@tec.ac.cr, isriom@estudiantec.cr, maxjimenez@tec.ac.cr, iaraya@tec.ac.cr , juan.montero@tec.ac.cr

Abstract— As the society energy demands continues to grow, it is increasingly important to improve the exploitation of renewable energy sources, such as wind energy. The strategies outlined in the literature show that there is an interest to enhance small-scale wind turbine performance. Small-scale wind turbines have been successfully installed in remote areas with no access to the electricity grids, and in distributed generation grids. To maximize the energy produced by wind turbines it is important to select the correct airfoil. The aerodynamic performance of a wind turbine is directly related to its energy production. This study aims at providing a complete experimental analysis on the SG6043 airfoil. The objective is to evaluate the aerodynamic behaviour of the proposed airfoil in 2D models, incorporating flow control devices such as flaps, vortex generators, and microtabs. Multiple tests have been run on the modified models of the airfoil in a wind tunnel. These tests aim to compare the drag and lift forces and the aerodynamic performance across all airfoil models. The analysis shown promising results as one of modifications reach up to 35% of dynamic performance increase compared to the nonmodified airfoil.

***Keywords*—Wind tunnel, airfoil, SG6043, flap, vortex generator, microtab, aerodynamic performance.**

I. Introduction

Energy can be seen as a determinant driving to human progress as it represents a fundamental need for development of civilizations [1]. The constant population growth around the world expands the energy demand for all type of applications, such as industry, commerce, transportation, and domestic use, among others [2]. The increasing demand of energy poses challenges to energy production. Particularly in the case of wind energy, as the best sites for wind farms on earth have been already exploited [3]. This challenge motivates the exploration of alternative ways to generate energy.

In this context, small-scale wind turbines have been already successfully installed in rural and urban areas around the world [4]-[5]. Although small-scale turbines are less efficient and have higher energy generation costs per kilowatt compared to large turbines, they present an interesting option for distributed generation grids. This is especially true in rural areas and wooded regions, where their unique advantages make them a practical and viable choice [6].

Exploiting energy in wooded areas and rural regions is not simple. Turbulence is often erratic, significantly affecting the turbine generation performance. There is a knowledge gap regarding the selection of suitable wind turbines for rural areas or wooded regions. For instance, [7] concluded that a small-scale wind turbine only achieved 37.75% of the 598kWh estimated using theoretical models. This gap has led to explore alternatives to enhance wind turbine performance.

There are multiple modifications that can be applied to airfoils to increase their performance. Geometrical modifications of the airfoil by using devices such as flaps, microtabs, vortex generators, suction equipment, synthetic jets and flexible walls, among others, have been proved to control aerodynamic effects on the airfoil [8]. Controlling the air flow around the airfoil may improve its energy generation performance [9].

It is possible to identify some research initiatives to improve the aerodynamic performance of airfoils by applying geometrical modifications. Flaps, microtabs and vortex generators are frequently mentioned in literature as common modifications to airfoils.

Flaps are components mounted on the trailing edge of the airfoil, designed to pivot through various angles for aerodynamic adjustment. The flap facilitates the transition from laminar to turbulent flow up to a certain point [8]. Studies, such as [10], have explored adaptive flaps to mitigate flow separation in wind turbines by varying flap length and placement. In [11], a flap of 10% chord length, tilted between 5° and 10°, demonstrated improved performance for small angles of attack. Better efficiency was observed when the flap was integrated into the geometry of the arifoil, eliminating edges that increase drag [12].

A microtab is a flow control device placed near the airfoil's trailing edge, projected to a right angle of it; also known with the name of Gurney flaps, they can improve the aerodynamic performance of aerodynamic airfoils, making them generate more lift and delaying the start of stall [13]. With a simple configuration, the microtabs allow great aerodynamic control and effectively increases rotor power coefficients [14]. The higher values in relations between lift coefficient and drag coefficient, according to [15] appeared when using microtabs, placed at 95% of the chord length, with height of 2% of the chord length, for a Reynolds number of 7×10^6. It was also noted that output power increases are more significant for low wind speeds when using microtabs.

The Vortex Generators (VG) were implemented for the first time in 1947, for aircraft control; VG are devices which, when fluid passes over them, generate concentrated vorticity, meaning eddies [16]. The fluid outside the high energy boundary layer is attracted to the boundary layer, injecting energy to the low energy fluid near the boundary layer, thus delaying its separation. In [17] it is shown how VG may effectively improve the lift coefficient of aerodynamic airfoil and control flow separation.

This paper aims to analyze the aerodynamic performance of a small-scale wind turbine airfoil by incorporating flaps, microtabs, and vortex generators. The selected airfoil is the SG6043, as it has been proved that it offers some advantages in aerodynamic performance for small-scale turbines [18]. This study emphasizes an experimental test conducted in a wind tunnel for each airfoil model. The airfoils maintain a consistent shape along their entire span, enabling their analysis as 2D models. Numeric analysis based on simulations and analysis on 3D rotors built form the proposed airfoil models are out of the scope of the current study. Therefore, the main objective of this study is to provide a rigorous guide of the effects that one or multiple geometrical modifications can have in the aerodynamic performance of a 2D airfoil.

II. Materials and Methods

To evaluate the aerodynamic performance of the SG6043 airfoil equipped with flow control devices, sixteen models were developed, incorporating various combinations of microtabs, flaps, and vortex generators. Eight models were constructed using polymer, while the remaining eight were fabricated from wood. Wind tunnel experiments were conducted to measure the lift and drag forces for each configuration. The data analysis process included the identification and exclusion of outliers, with measurements repeated as needed to ensure statistical consistency. This approach adhered to best practices in experimental methodology, minimizing potential errors associated with operator performance.

A. *Airfoils*

All airfoils in this study are based on the SG6043 geometry, with its 2D distribution detailed in [19]. The dimensions of the models used are a chord length of 0.15 m and an airfoil width of 0.15 m. These dimensions comply with the maximum blockage factor of 10% of the wind tunnel's cross-sectional area, as specified in [20]. Additionally, the experiments achieved a Reynolds number on the order of 10^5, which is relevant for small-scale wind turbines, as indicated in [21].

Regarding the flow control devices, the microtabs have a height of 2% of the chord length, a width of 1% of the chord length, and are positioned at 95% of the chord. The flaps are 10% of the chord length and are inclined at an angle of 10°. The vortex generators (VGs) have a height and width of 2% of the chord length and are located at 20% of the chord. All control devices have the same shape along their entire span. Fig. 1 shows a sample of four airfoils developed for this study. At upper left part it is shown the unmodified airfoil, next to a model equipped with a flap. At the lower part of Fig. 1 two models are shown, one with VG (shown upside down to evidence the shape of the VG) and another with microtab.

Fig. 1. Airflow control devices on a sample of airfoil models.

Considering these three flow control devices, airfoil models were constructed from wood and polymer (PETG - Polyethylene Terephthalate Glycol Modified). Eight airfoils were built from each material, with different combinations of the flow control devices, as outlined in Table I. The airfoils are coded with the letter "M" for wood and "P" for polymer. Fig. 2 illustrates the sixteen airfoils developed for this research. The "Xs" in Fig. 2 are replaced by "M" and "P" on Table I depending on the material.

For the fabrication of the PETG aerodynamic airfoils, the Fused Deposition Modeling (FDM) process was used with a 3D Cartesian printer model "Artillery Sidewinder X1." The filament had a diameter of 1.75 ± 0.05 mm, with a printing temperature of 180°C, a bed temperature of 80°C, a layer height of 0.16 mm, line thickness of 0.4 mm, 4 perimeters, 25% infill, and an overall printing speed of 45 mm/s.

For the manufacturing of the MDF (Medium Density Fiberboard) aerodynamic airfoils, 3 mm-thick sheets were used, which were laser-cut and then assembled with white glue, reaching a width of 150 mm in the airfoils. Additionally, two 3/8-inch steel rods were employed to align the sheets, providing structural support. To eliminate any surface imperfections, the airfoils went through a sanding process.

B. *Wind tunnel testing*

Once the 16 airfoils were prepared, lift and drag force tests were conducted in the wind tunnel shown in Fig. 3, located at LIENE (Laboratorio de Investigación en Energía Eólica) at the Tecnológico de Costa Rica. The wind tunnel is equipped with a Pitot 160F tube, an AFA5 transducer for measuring pressure differences, and an AF1300z balance to measure lift and drag forces. Data was collected and recorded using the VDAS-B MKII data acquisition system.

The Pitot tube has an accuracy of 2% and a coefficient of 0.81. The AFA5 transducer has a measurement range from 0 kPa to 7 kPa, with calibration performed by the supplier. The AF1300z balance is designed to support a maximum load of 10 kg (100 N) and is calibrated using standard weights ranging from 1 to 500 g.

TABLE I
CODIFICATION OF AERODYNAMIC AIRFOILS

Code	Material	Microtab	Flap	VG
M1	Wood			
M2	Wood	X		
M3	Wood		X	
M4	Wood			X
M5	Wood	X	X	
M6	Wood	X		X
M7	Wood		X	X
M8	Wood	X	X	X
P1	Polymer			
P2	Polymer	X		
P3	Polymer		X	
P4	Polymer			X
P5	Polymer	X	X	
P6	Polymer	X		X
P7	Polymer		X	X
P8	Polymer	X	X	X

The wind tunnel at LIENE features a transverse test section that narrows from 300x300 mm to 275x275 mm, where the aforementioned equipment is located. The tunnel is equipped with a Greenheck TDI 6-blade axial fan, powered by a Toshiba EQP Global SD 1 HP motor, controlled by a Toshiba VF-S15 frequency inverter. The system allows a minimum frequency of 880 RPM and a maximum of 1800 RPM, corresponding to wind speeds ranging from 7 m/s to 15 m/s, respectively. Fig. 4 illustrates the experimental setup for the tests, with the airflow moving from right to left along the Y-axis, as shown in the figure.

For each airfoil, lift and drag forces were measured for Angles of Attack (AoA) ranging from -25° to 50°, in increments of 5°. The test order was randomized. A wind speed of 10.5 m/s was used, with the average air kinematic viscosity in the laboratory being 1.516×10^{-5} m²/s, resulting in a Reynolds number of 1.04×10^{5}, based on a chord length of 0.15 m. The sampling time was set to 60 seconds with a frequency of 2 Hz, resulting in 120 measurements at each angle of attack. A summary of the experimental design is provided in Table II. As the set up for each test is identical, no wind tunnel wall corrections were applied. The measured forces on each test allow to compare the effect of each control flow device equipped on the airfoil.

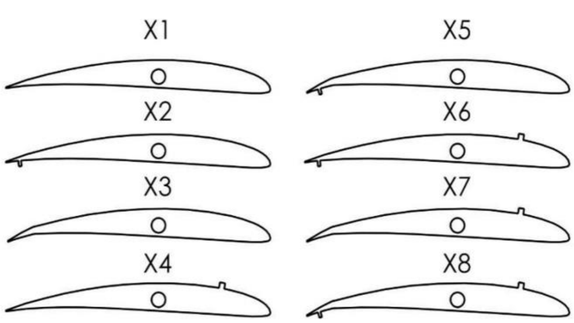

Fig. 2. Airfoils with flow control devices


Fig. 3. Wind tunnel.

B. Data Processing

For the 120 measurements at each position, the average value and its associated variance are calculated. Samples with bias due to human error are identified and excluded. The results are presented using a box plot and a histogram. The box plot is used to determine the distribution of the samples, while the histogram allows for the comparison of their distributions [22]. The graphics are generated using the Python Matplotlib library.

An expected outcome from the graphics is a Gaussian distribution for lift and drag forces. Therefore, it is anticipated that values with minimal error or bias will cluster closely around the average [22]. To achieve this, it is determined that samples with overlaps in their second or third quartile can be grouped, with the goal of identifying the group with the largest number of samples.

If the samples do not overlap in the second or third quartile, a search of overlap in any of their quartiles is performed, particularly the central quartile. This aims at mitigating biases by grouping a larger amount of data.

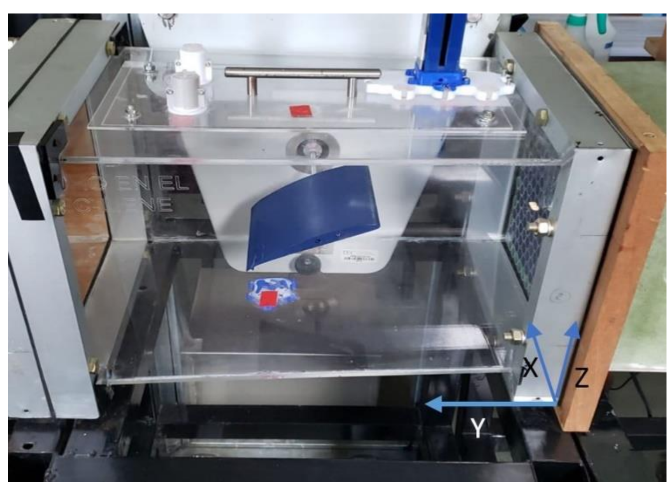

Fig. 4. Experimental set up for airfoils test.

TABLE II

SUMMARY OF THE EXPERIMENTAL DESIGN

Parameter	Description of possible test	Possible tests
Material	Wood or Polymer	2
Flow control device	SG6043 airfoil base, equipped with flaps, microtabs and VG. Possible combinations as shown on Table I	8
Angle of attack	From -25° to 50°, in increments of 5°.	16
Iterations	Three iterations per test	3
Total of tests		768

Samples that do not overlap in any of their quartiles, or in their outer quartiles, will be considered erroneous and rejected from the consolidated dataset. If multiple valid groups with different locality are found, data collection for that airfoil will be repeated. Additionally, for each set of samples, atypical data points more than 1.5 times the interquartile range away from the average are removed.

III. RESULTS AND DISCUSSION

The results are initially grouped based on the airfoil material, with the wooden (M) airfoils analyzed first, followed by the polymer (P) airfoils. For each material, the results of are presented on three different graphics. The first graphic presents the lift forces versus the angle of attack, the second graphic presents the drag force versus the angle of attack, and the third graphic presents the lift-to-drag ratio (L/D) versus the angle of attack. It is important to recall that 16 different positions of angle of attack were tested. The L/D graphic shows the best results for each material.

A. M airfoils

An analysis of the results for wooden airfoils, as shown in Fig. 5 and Fig. 6, reveals a consistent trend across all models for both lift and drag curves. Airfoils M2, M3, and M5 stand out with better lift performance at positive angles of attack, while airfoils M7 and M8 demonstrate superior lift at negative angles.

Airfoils with microtabs positioned on the upper surface do not enhance lift at positive angles of attack, likely due to the microtabs promoting boundary layer separation as the angle of attack increases. In contrast, at negative angles of attack, the combination of the elevated microtab and the flap significantly improves lift.

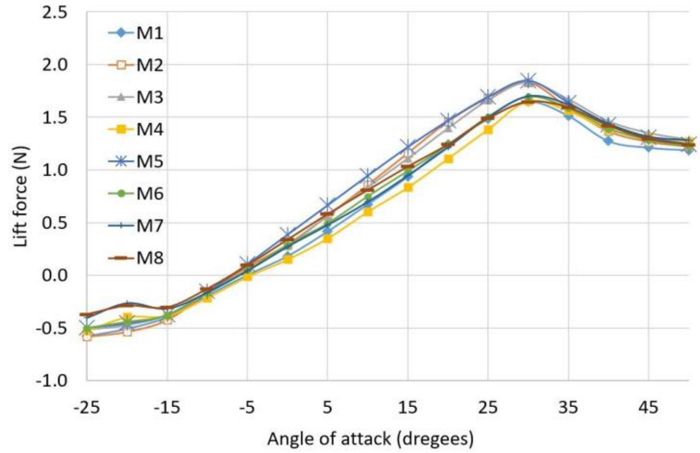

Fig. 5. Lift force for wood airfoils (M).

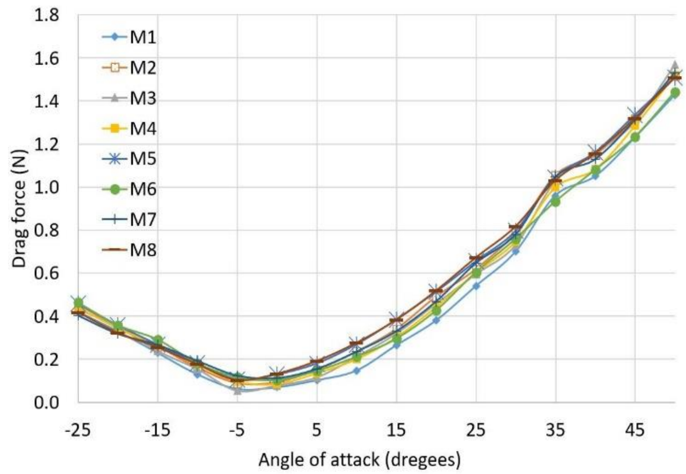

Fig. 6. Drag forces for wood airfoils (M).

The drag versus angle of attack curve shows that the unmodified airfoil has the best results in terms of aerodynamic performance. The airfoils M7 and M8 show the greatest wind resistance among the studied models. This demonstrates that the incorporation of airflow control devices such as flaps, microtabs and VG, increases the drag forces on the airfoil.

When analysing the lift-to-drag curve (Fig. 7) and focusing on the airfoils with the best ratios, airfoil M3 stands out, featuring only one flap. A point-by-point comparison between the unmodified SG6043 airfoil and M3 reveals differences of 35% and 20% in favour of M3 at angles of attack of 0° and 5°, respectively, aligning with previous findings reported in the literature [11].

On the other hand, differences of 16% and 7% favor the base airfoil at angles of attack of 10° and 20°, respectively. When comparing both curves and calculating the point-by-point average difference by subtracting M3 values from the values of the unmodified SG6043, a positive average of 0.18 is obtained. This indicates that, on average, airfoil M3 achieves a better L/D ratio than the unmodified airfoil. The difference is particularly

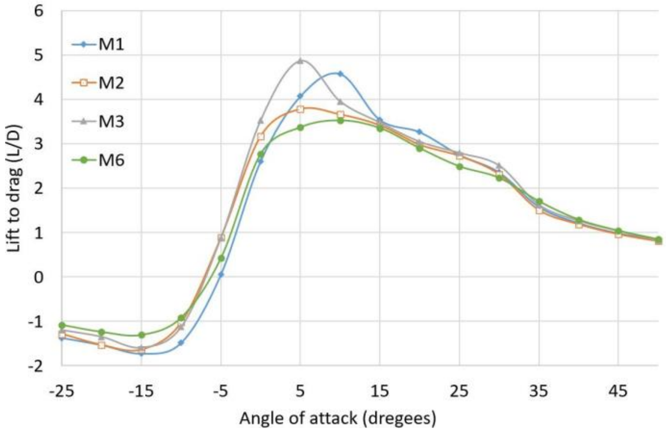

Fig. 7. Lift/drag ratio for wood airfoils (M).

notable at the point where both airfoils, M3 and the base SG6043, reach their maximum L/D ratio.

Considering the presented results, it can be concluded that the SG6043 airfoil with one flap, as proposed in airfoil M3, offers better average aerodynamic performance than the base SG6043 under conditions with Re = 10^5, as observed in this study and reported in the literature. This performance improvement is associated with the formation of a laminar separation bubble [21], which negatively impacts the efficiency of small-scale wind turbines operating in turbulent flow. Therefore, the addition of this flap is determined to enhance performance under turbulent conditions.

B. *P Airfoils*

Regarding lift curve in polymer airfoils (Fig. 8), airfoils equipped with an upper microtab (P4, P6, P7, and P8) show lower performance compared to the others. However, among the airfoils equipped with upper microbats, P7 and P8 present some lift improvements at negative angles of attack. At positive angles of attack, there is no evidence of lift improvement for any of the modification on the SG6043 airfoil.

For drag curve (Fig. 9), the unmodified airfoil consistently exhibits the lowest drag across most of the studied range. Airfoils with upper microtabs (P4, P6, P7, and P8) maintain their trend of greater aerodynamic resistance.

Examining the lift-to-drag curves for polymer airfoils (Fig. 10), airfoil P2 shows a better response than the base airfoil at certain non-consecutive angles of attack. Airfoil P3, featuring a flap, demonstrates improved performance among the modified airfoils but does not surpass the results of the unmodified airfoil.

A comparison of Fig. 7 and Fig. 10 reveals that airfoils 2 (model using lower microtab) and 3 (model using flap) outstand the best average results for both wood and polymer materials. However, when evaluating the flow control devices against the unmodified SG6043 airfoil, it is evident that only at angles of attack of 0° and -15°, airfoil P2 offers a significant improvement over the unmodified SG6043. In contrast, airfoil M3 provides better overall performance on average compared to the unmodified airfoil. Therefore, it can be concluded that while microtabs improve aerodynamic performance at specific angles of attack, flaps offer a consistent and stable improvement in a larger range of the studied angles of attack. It is important to mention that none of the flow control devices consistently increase the L/D ratio along the whole range of studied angles of attack.

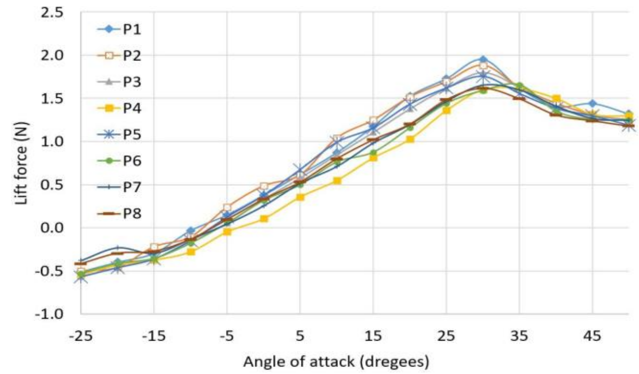

Fig. 8. Lift forces for polymer airfoils (P).

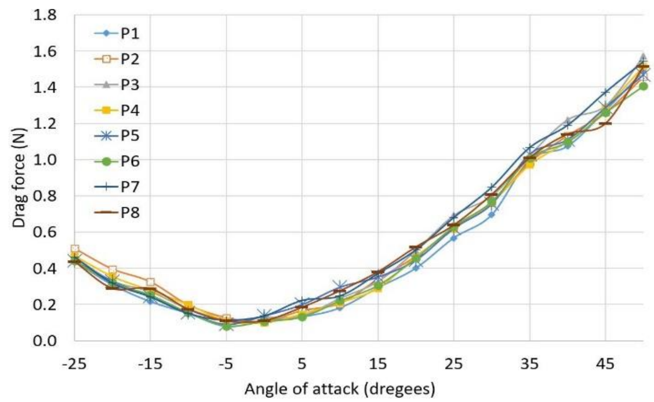

Fig. 9. Drag forces for polymer airfoils (P).

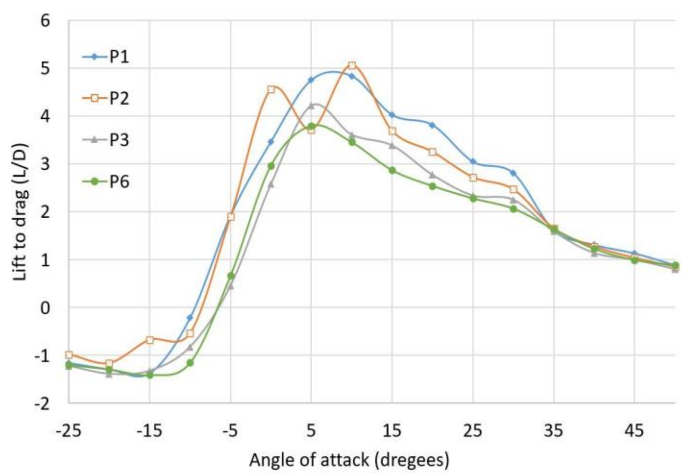

Fig. 10. Lift/drag ratio for polymer airfoils (P).

IV. CONCLUSIONS

Considering the effects of various flow control devices, such as flaps, vortex generators (VG), and microtabs, on the SG6043 airfoil at a Reynolds number of 10^5, the following conclusions can be drawn:

- None of the flow control devices consistently increase the lift-to-drag ratio across all angles of attack.
- A single flap, sized at 10% of the chord and angled at 10°, can improve the aerodynamic performance of the SG6043 airfoil on average, with improvements reaching up to 35% at an angle of attack of 0°.
- Flow control devices show favorable effects primarily at small angles of attack (10° or less). This finding is consistent with prior research found in the literature of similar studies.
- Vortex generators enhance the lift-to-drag ratio at negative angles of attack.

While no modified airfoil proves consistently superior to the base SG6043 airfoil across the full range of angles of attack analyzed, the results indicate that flaps may enhance performance at specific angles. Future work perspectives are oriented to build and test a rotor with the proposed flaps in this study. Three-dimensional effects in rotor applications extend beyond the scope of this two-dimensional study. A three-dimensional model will allow to assess the impact of the flaps on the power coefficient under real operational conditions.

ACKNOWLEDGEMENTS AND DECLARATION OF AUTHOR CONTRIBUTIONS

The authors acknowledge the collaboration in this research of Luis Diego Murillo, Gustavo Murillo Zumbado, Iván Araya Meneses, and the assistants of LIENE at the Tecnológico de Costa Rica. We also thank the same institution for funding the development of this research through project VIE 1341020.

The researchers declare that the contribution in this document is as follows: GRN 15%, IBC 15%, IAM 15%, MJC 15%, and JJMJ 40%.

REFERENCES

[1] L. Guruswamy, "Energy justice and sustainable development," *Colo. J. Int'l Envtl. L. & Pol'y*, vol. 21, pp. 231, 2010.

[2] K. Kodeeswara and P. Parthiban, "Performance analysis of micro wind turbine-based energy systems with series connected inverters and a novel switching network," *Journal of Green Engineering*, pp. 385–400, 2017.

[3] S. Mertens, *Wind energy in the built environment: concentrator effects of buildings*, Ph.D. dissertation, Technische Universiteit Delft, Brentwood, United Kingdom, 2006.

[4] G. Alkawsi, Y. Baashar, A. Alkahtani, C. W. Lim, S. K. Tiong and M. Khudari, "Viability assessment of small-scale on-grid wind energy generator for households in Malaysia" Energies 14 (12), 2021. https://doi.org/10.3390/en14123391

[5] J. Zalewska, K. Damaziak and J. Malachowski, " An energy efficiency estimation procedure for small wind turbines at chose locations in Poland" Energies, 14 (12), 2021. https://doi.org/10.3390/en14123706

[6] IEA-ETSAP and IRENA, "Wind Power Technology Brief," Technology Brief E07, 2016.

[7] K. Torres, C. Torres and G. Richmond-Navarro. Microgeneración de energía eólica en un entorno boscoso en Costa Rica: estudio de caso. Tecnología en Marcha 61-69, 2020

[8] K. Xu and G. Zha, "High efficiency wind turbine using co-flow jet active flow control," Proceedings of ASME Turbo Expo 2021, pp. 1–15, 2021.

[9] S. Thakur, K. Abhinav, and N. Saha, "Load mitigation using slotted flaps in offshore wind turbines," Journal of Offshore Mechanics and Arctic Engineering, 2018. https://doi.org/10.1115/1.4040234

[10] W. Haoa, M. Bashir, C. Li, and C. Sum, "Flow control for high-solidity vertical axis wind turbine based on adaptive flap," Energy Conversion and Management, vol 249, 2021. https://doi.org/10.1016/j.enconman.2021.114845

[11] X. Bofeng, J. Junheng, L. Qing, X. Chang, Z. Zhenzhou, and Y. Yue, "Aerodynamic performance analysis of a trailing-edge flap for wind turbines" Journal of Physics: Conference Series, Vol 1037, issue 2, 2018. DOI 10.1088/1742-6596/1037/2/022020

[12] M. Castillo-Acero, C. Cuerno-Rejado, and M. Gomez-Tierno, "Morphing structure for a rudder" The Aeronautical Journal, vol 120, issue 1230, pp. 1291–1314, 2016. DOI: https://doi.org/10.1017/aer.2016.54

[13] A. Bianchini, F. Balduzzi, D. Di Rosa, and G. Ferrara, "On the use of Gurney flaps for the aerodynamic performance augmentation of Darrieus wind turbines", Energy conversion and management, vol 184, pp 402-415, 2019. https://doi.org/10.1016/j.enconman.2019.01.068

[14] Y. Zhang, V. Ramdoss, Z. Saleem, X. Wang, G. Schepers, and C. Ferreira, "Effects of root Gurney flaps on the aerodynamic performance of a horizontal axis wind turbine," Energy, vol 187, 2019. https://doi.org/10.1016/j.energy.2019.115955

[15] U. Fernandez-Gamiz, E. Zulueta, A. Boyano, J. Ramos-Hernanz, and J. Lopez-Guede, "Microtab design and implementation on a 5 MW wind turbine," Applied Sciences 7(6), 536, 2017. https://doi.org/10.3390/app7060536

[16] X. Li, K. Yang, and X. Wang, "Experimental and numerical analysis of the effect of vortex generator height on vortex characteristics and airfoil aerodynamic performance," Energies, pp. 1–19, 2019. https://doi.org/10.3390/en12050959

[17] H. Wang, B. Zhang, Q. Qui, and X. Xu, "Flow control on the NREL S809 wind turbine airfoil using vortex generators" Energy, vol 118, pp. 1210–1221, 2017. https://doi.org/10.1016/j.energy.2016.11.003

[18] M. Montenegro and G. Richmond, "Simulación del desempeño de tres perfiles aerodinámicos en flujo turbulento," Universidad, Ciencia y Tecnología, pp. 212–225, 2021.

[19] SG6043, "SG6043 (sg6043-il)," available: http://airfoiltools.com/airfoil/ details? Airfoil=sg6043-il.

[20] J. Barlow, W. H. RAE, JR, and A. Pope "Low speed wind tunnel testing" Third edition, John Wiley and Sons, 1999. ISVN 0-471-55774-9

[21] Q. Li, Y. Kamada, T. Maeda, J. Murata, and Y. Yusuke, "Effect of turbulence on power performance of a horizontal axis wind turbine in yawed and no-yawed flow conditions", Energy, vol 109, pp 703-711, 2016. https://doi.org/10.1016/j.energy.2016.05.078

[22] R. E. Walpole and R. H. Myers, "Probabilidad y Estadística para Ingenieros" novena edición, Pearson education, México, 2012. ISBN 978-607-32-1417-9